INT. J. CONTROL, 1989, VOL. 50, NO. 5, 1699–1715

# Trajectory control of a non-linear one-link flexible arm

ALESSANDRO DE LUCA† and BRUNO SICILIANO‡

The trajectory-tracking control problem is considered for a one-link flexible arm described by a non-linear model. Two meaningful system outputs are chosen; namely, the joint angle and the angular position of a suitable point along the link. The common goal is to stiffen the behaviour of the flexible link with respect to the chosen output. Based on the input–output inversion algorithm, a state-feedback control law is designed that enables exact tracking of any smooth trajectory specified for the output. In the closed loop an unobservable dynamics naturally arises, related to the variables describing the arm's distributed flexibility. Joint-based design is shown to be always stable, whereas in the link-point design the closed-loop dynamics may become unstable depending on the location of the output along the link. Open- versus closed-loop strategies are developed and compared. Extensive simulation results are included.

## 1. Introduction

Robots are typically asked to perform continuous tasks such as arc welding, spray painting, laser cutting and deburring. These applications demand that the robot controller be capable of accurately reproducing pre-planned smooth trajectories (Engelberger 1980). This accuracy is guaranteed by current industrial robots at the expense of a rigid and massive mechanical design.

Recently, the adoption of lightweight flexible arms has been proposed as offering potential benefits like increased payload-to-arm ratio, faster executable motions and lower energy consumption (Book 1984). In spite of these advantages, the control problem of robots having flexible members becomes much more complex. If high performance is desired, an accurate dynamic model is strictly required by the controller.

Most of the existing control approaches use classical methods based upon linear models, either for designing a regulator around a target point (Hastings and Book 1985, Cannon and Schmitz 1986) or for performing trajectory tracking (Bayo 1987). Other works utilize non-linear models and different approximate control techniques such as adaptive control (Siciliano *et al.* 1986), pseudo-linearization (Nicosia *et al.* 1989) or singular perturbation (Siciliano and Book 1988).

For rigid non-redundant robot arms, it is known that the controlled variables may be equivalently defined both in the task space and in the joint or actuator space (Craig 1986). On the other hand, establishing the control objectives to be pursued in the case of flexible arms is a critical issue. One might be interested in regulating the end-point around a final position, or in tracking joint trajectories while limiting arm deflections,

Received 24 May 1988. Revised 2 December 1988.

† Dipartimento di Informatica e Sistemistica, Università degli Studî di Roma, 'La Sapienza', Via Eudossiana 18, 00184 Roma, Italy.

‡ Dipartimento di Informatica e Sistemistica, Università degli Studî di Napoli, 'Federico II', Via Claudio 21, 80125 Napoli, Italy.

0020-7179/89 $3.00 

or even in driving the end-point along a feasible path. Therefore, the system output has to be chosen according to the specified control goal.

In this paper, a non-linear control law is designed using the input–output inversion algorithm (Hirschorn 1979) in order to achieve exact trajectory tracking for a certain class of outputs. Similarly to most of the contributions in the field, the proposed control method is developed for the one-link flexible arm as a first step towards general multi-link arms. In any case, the non-linear dynamic terms are here explicitly taken into account in the model.

In particular, two alternative system outputs are considered for trajectory tracking. A first natural choice is the joint angle, similar to the rigid-arm case. A second possibility is to pick up a suitable point along the flexible link and choose as output its angular position with respect to a fixed reference frame.

The inversion approach was first used by Singh and Schy (1984) for rigid-arm control and it corresponds to the well-known computed torque method of Bejczy (1974). The same technique has also been applied successfully to robot arms with elasticity concentrated at the joints (De Luca 1988). The most relevant result of using inversion-based feedback control for these two classes of robot arm is the equivalence of the obtained closed-loop system to a linear and decoupled one, i.e. to strings of input–output integrators.

However, when the same technique is applied to flexible arms, the full linearization property is lost. In the closed loop, a subsystem arises which becomes unobservable and possibly non-linear. As a matter of fact, this subsystem describes the behaviour of the elastic variables associated with the arm deformation. Its dynamic characteristics depend on the particular output chosen and stability has to be ensured in order to validate the overall control design. If this is the case, it can be concluded that the flexible link has been stiffened under feedback with respect to that output.

It will be shown that when the output is chosen to be the joint angle, the closed-loop dynamics is always stable (De Luca and Siciliano 1988). The same result does not necessarily hold when selecting as output the angular position of a point along the link. In that case, it will be possible to find that particular location on the arm beyond which the inversion-based technique for trajectory reproduction leads to an unstable design, as suggested by De Luca *et al.* (1988). Thus, in general, end-point trajectories cannot be tracked exactly without going unstable.

Two possible implementation schemes of the control laws obtained via the system-inversion technique are developed. A *closed-loop* strategy requires non-linear static feedback from the full state of the arm. On the other hand, pre-computation of *open-loop* torques driving the output angle on a given trajectory asks for the off-line integration of a reduced-order dynamic system. This yields the behaviour of the arm deflection associated with the desired output trajectory.

The paper is organized as follows. Section 2 presents the dynamic equations of a one-link flexible arm modelled using the assumed mode technique. In § 3, open- and closed-loop joint-based control laws are derived and their stability properties are briefly analysed. The tracking controller for the angular position of a point on the link is developed in § 4. Section 5 contains the results of a simulation study that allows for a comparison of the above control strategies on the basis of the induced end-point deflections. Conclusions are drawn in the final section.

## 2. Dynamic model of the flexible link

The one-link flexible arm of Fig. 1 is considered. The arm moves on a horizontal plane and does not undergo torsional deformations. The link is modelled as an

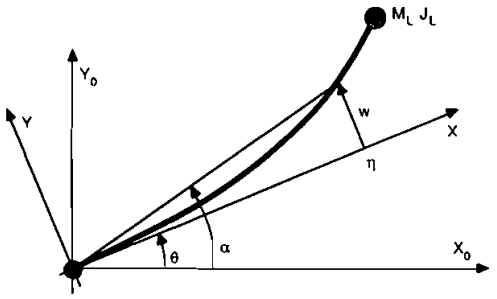


Figure 1. One-link flexible arm.

Euler–Bernoulli beam having the equation

$$EI\frac{\partial^4 w(\xi, t)}{\partial \xi^4} + \rho AL^4 \frac{\partial^2 w(\xi, t)}{\partial t^2} = 0$$

where $\xi = \eta/L$ is the normalized position along the link of length $L$, $A$ is the link cross-sectional area and $I$ its inertia, $E$ is the Young's modulus of the material and $\rho$ its uniform density. Assuming separability in time and space, i.e.

$$w(\xi, t) = \phi(\xi)\delta(t)$$

modal analysis gives the following general solution (Meirovitch 1967)

$$\delta(t) = \exp(j\omega t) \quad \omega^2 = \frac{\beta^4 EI}{\rho AL^4}$$

$$\phi(\xi) = C_1 \sin(\beta\xi) + C_2 \cos(\beta\xi) + C_3 \sinh(\beta\xi) + C_4 \cosh(\beta\xi)$$

The boundary conditions to the problem specify an infinite set of admissible values for the parameter $\beta$, each of which determines an associated eigenfrequency $\omega$ of the beam.

The following clamped-mass boundary conditions are imposed on the eigenfunction $\phi(\xi)$:

clamped:

$$\phi(\xi)|_{\xi=0} = 0 \quad \left.\frac{d\phi(\xi)}{d\xi}\right|_{\xi=0} = 0$$

mass:

$$\left.\frac{d^2\phi(\xi)}{d\xi^2}\right|_{\xi=1} = \frac{J_L\beta^4}{\rho AL^3}\left.\frac{d\phi(\xi)}{d\xi}\right|_{\xi=1}$$

$$\left.\frac{d^3\phi(\xi)}{d\xi^3}\right|_{\xi=1} = -\frac{M_L\beta^4}{\rho AL}\phi(\xi)|_{\xi=1}$$

where $M_L$ and $J_L$ are, respectively, the load mass and the load inertia. The clamped conditions at the joint yield

$$C_3 = -C_1 \quad C_4 = -C_2$$

while the mass conditions at the end-point lead to

$$[Q(\beta)]\begin{bmatrix} C_1 \\ C_2 \end{bmatrix} = 0$$

where the so-called frequency equation is given by setting to zero the determinant of the $2 \times 2$ matrix $Q(\beta)$. It can be shown that the positive values of $\beta$ are given by the solutions of the transcendental equation

$$(1 + \cos\beta \cosh\beta) - M\beta(\sin\beta \cosh\beta - \cos\beta \sinh\beta) - J\beta^3(\sin\beta \cosh\beta + \cos\beta \sinh\beta) + MJ\beta^4(1 - \cos\beta \cosh\beta) = 0$$

where $M = M_L/\rho AL$ and $J = J_L/\rho AL^3$.

By considering a finite number $m$ of modal terms, the dynamic equations for the one-link flexible arm are derived following a lagrangian approach (Siciliano and Book 1988) in the form

$$B(\delta)\begin{bmatrix}\ddot{\theta}\\ \ddot{\delta}\end{bmatrix} + \begin{bmatrix}n_1(\dot{\theta}, \delta, \dot{\delta})\\ n_2(\dot{\theta}, \delta)\end{bmatrix} + \begin{bmatrix}0\\ K\delta + F\dot{\delta}\end{bmatrix} = \begin{bmatrix}u\\ 0\end{bmatrix}$$

where $\theta$ is the joint variable, $\delta = [\delta_1 \quad \dots \quad \delta_m]^T$ is the vector of modal amplitudes, and $u$ is the control torque at the joint location.

The elements $b_{ij}$ of the positive-definite symmetric inertia matrix $B(\delta)$ take on the expressions below, which are valid when clamped-free modes are used in the presence of a tip payload. Similar expressions hold if a mismatch exists between the actual and the assumed boundary conditions at the tip:

$$b_{11}(\delta) = J_0 + J_L + M_L L^2 + I_0 + M_L(\Phi_e^T\delta)^2$$

$$b_{1j} = M_L L\phi_{j-1,e} + J_L\phi'_{j-1,e} + \sigma_{j-1}, \quad j = 2, \dots, m+1$$

$$b_{ii} = m_b + M_L\phi^2_{i-1,e} + J_L\phi'^2_{i-1,e}, \quad i = 2, \dots, m+1$$

$$b_{ij} = M_L\phi_{i-1,e}\phi_{j-1,e} + J_L\phi'_{i-1,e}\phi'_{j-1,e}, \quad i = 2, \dots, m+1, \quad j \neq i$$

with

$$\Phi_e^T = \Phi^T|_{\xi=1} = [\phi_1 \quad \dots \quad \phi_m]|_{\xi=1} \quad \phi_{ie} = \phi_i(\xi)|_{\xi=1}$$

$$(\Phi'_e)^T = [\phi'_{1e} \quad \dots \quad \phi'_{me}] \quad \phi'_{ie} = \left.\frac{d\phi_i(\xi)}{d\xi}\right|_{\xi=1}$$

$$\sigma_i = \rho AL^2 \int_0^1 \phi_i(\xi)\xi \, d\xi \quad i = 1, \dots, m$$

where $m_b$ is the link mass, $I_0$ is the joint actuator inertia, and $J_0$ is the link inertia relative to the joint.

The non-linear terms $n_1$ and $n_2$ can be computed by differentiation of the elements of the inertia matrix and represent Coriolis and centrifugal terms:

$$n_1(\dot{\theta}, \delta, \dot{\delta}) = 2M_L\dot{\theta}(\Phi_e^T\delta)(\Phi_e^T\dot{\delta})$$

$$n_2(\dot{\theta}, \delta) = -M_L\dot{\theta}^2(\Phi_e\Phi_e^T)\delta$$

$K$ is an equivalent-spring constant matrix

$$K = \text{diag}\{k_1, \dots, k_m\}$$

$$k_i = \frac{EI}{L^3}\int_0^1 \left[\frac{d^2\phi_i(\xi)}{d\xi^2}\right]^2 d\xi$$

$F$ is a damping matrix

$$F = \text{diag}\{f_1, \dots, f_m\}$$

which accounts for the internal viscous friction in the flexible structure. It should be mentioned that the enhancement of such a passive damping is a feasible alternative to active modal control (Book *et al.* 1985).

Notice that no control input appears in the left-hand side of the lower $m$ dynamic equations, as a result of the clamped assumption for the flexible link. Also, the arm model is independent from the joint angle value $\theta$, owing to the symmetry of system dynamics around the joint axis.

In the following, the inverse $D(\delta)$ of the system inertia matrix will be used. $B(\delta)$ can be conveniently partitioned into four blocks

$$B(\delta) = \begin{bmatrix} b_{11}(\delta) & B_{12}^{\mathrm{T}} \\ B_{12} & B_{22} \end{bmatrix}$$

with $B_{22}$ of order $m \times m$. Accordingly, the inverse can be written explicitly as

$$D(\delta) = B^{-1}(\delta) = \begin{bmatrix} d_{11}(\delta) & D_{12}^{\mathrm{T}}(\delta) \\ D_{12}(\delta) & D_{22}(\delta) \end{bmatrix}$$

with

$$d_{11}(\delta) = \frac{1}{b_{11}(\delta) - B_{12}^{\mathrm{T}} B_{22}^{-1} B_{12}}$$

$$D_{12}(\delta) = -\frac{\Delta^{-1}(\delta) B_{12}}{b_{11}(\delta)} \qquad D_{22}(\delta) = \Delta^{-1}(\delta)$$

and

$$\Delta(\delta) = B_{22} - \frac{B_{12} B_{12}^{\mathrm{T}}}{b_{11}(\delta)}$$

## 3. Joint-based inversion control

Once a scalar output $y$ is associated with the flexible-arm system, the input torque $u$ that is capable of exactly reproducing a given trajectory $y_d(t)$ can be derived by means of system-inversion techniques. A joint-based strategy is pursued first. The derivation of the control law in this case follows directly from (De Luca and Siciliano 1988). The output is chosen as

$$y = \theta$$

Applying the inversion algorithm of Hirschorn (1979), it is easy to see that the input $u$ explicitly appears in the second derivative of the output function

$$\ddot{y} = d_{11}(\delta)[u - n_1(\dot{\theta}, \delta, \dot{\delta})] - D_{12}^{\mathrm{T}}(\delta)[n_2(\dot{\theta}, \delta) + K\delta + F\dot{\delta}]$$

Since $d_{11}(\delta) \neq 0$ always, this is true no matter what flexible arm is considered or how many modes are assumed.

Let $a = a(t)$ be the desired output acceleration. Then, the input–output linearizing control torque can be obtained by setting

$$\ddot{y} = a$$

in the above equation. Solving for $u$ gives

$$u = n_1(\dot{\theta}, \delta, \dot{\delta}) + \frac{1}{d_{11}(\delta)}[a + D_{12}^{\mathrm{T}}(\delta)(n_2(\dot{\theta}, \delta) + K\delta + F\dot{\delta})]$$

$$= u^*(a, \dot{\theta}, \delta, \dot{\delta})$$

The input torque $u^*$ is the one that 'stiffens' the motion of the flexible arm at the joint location, ensuring the tracking of any desired output trajectory. Indeed, exact reproduction is guaranteed only if the trajectory is of class $C^1$ (i.e. with, at most, step discontinuities in acceleration) and if there is matching with the initial conditions, in this case with joint position and velocity. Otherwise, only asymptotic tracking is obtained.

The above control law can be implemented in an open- or in a closed-loop scheme. Assume that a desired smooth joint trajectory $\theta = \theta_d(t)$ has been given, together with its time derivatives.

### 3.1. *Open-loop control*

In this scheme set

$$\dot{\theta} = \dot{\theta}_d(t) \quad a = \ddot{\theta}_d(t)$$

The control $u^*$ is not completely specified by these identities, since knowledge of $\delta(t)$ and $\dot{\delta}(t)$ is still needed. This is essentially different from the case of rigid arms, where assigning the behaviour to the joint variables uniquely determines the required torque inputs. Here, a dynamic generator has to be set up to recover the time evolution of the elastic coordinates $\delta$. Plugging the expression for $u^*$ into the dynamic equations and replacing the joint variables by their desired values gives

$$\ddot{\delta} = -B_{22}^{-1}[B_{12}\ddot{\theta}_d + n_2(\dot{\theta}_d, \delta) + K\delta + F\dot{\delta}]$$

The off-line integration of these $m$ second-order differential equations, starting from $(\delta(0), \dot{\delta}(0))$, yields the desired time evolutions $(\delta_d(t), \dot{\delta}_d(t))$. If the above dynamics were unstable, the whole process of generation of the open-loop torque would be unfeasible. Note that these differential equations are *linear* time-varying ones and can be rewritten in state-space format as

$$\begin{bmatrix} \dot{\delta} \\ \ddot{\delta} \end{bmatrix} = \begin{bmatrix} \mathbf{0} & \mathbf{I} \\ A_{21}(\dot{\theta}_d) & A_{22} \end{bmatrix} \begin{bmatrix} \delta \\ \dot{\delta} \end{bmatrix} + \begin{bmatrix} \mathbf{0} \\ b_2(\ddot{\theta}_d) \end{bmatrix} = A(t) \begin{bmatrix} \delta \\ \dot{\delta} \end{bmatrix} + b(t)$$

with

$$A_{21}(\dot{\theta}_d) = -B_{22}^{-1}[K - M_L\dot{\theta}_d^2(\Phi_e\Phi_e^T)]$$
$$A_{22} = -B_{22}^{-1}F \quad b_2(\ddot{\theta}_d) = -B_{22}^{-1}B_{12}\ddot{\theta}_d$$

The resulting open-loop torque to be applied at the joint is then

$$u_{OL} = u^*(\ddot{\theta}_d, \dot{\theta}_d, \delta_d, \dot{\delta}_d)$$

To gain some robustness at low expense, a linear feedback can be used in addition to this reference torque signal. A proportional derivative (PD) controller on the joint-trajectory error is properly designed as

$$u_{OL,PD} = u^*(\ddot{\theta}_d, \dot{\theta}_d, \delta_d, \dot{\delta}_d) + \frac{1}{d_{11}(\delta_d)}[k_p(\theta_d - \theta) + k_v(\dot{\theta}_d - \dot{\theta})]$$

It is worth remarking that this kind of control law does not require any measurement of arm deflection.

3.2. *Closed-loop control*

In this case $u^*$ is computed by feeding back the full state $(\theta, \dot{\theta}, \delta, \dot{\delta})$ of the flexible arm. The resulting closed-loop system equations are given by

$$\ddot{\theta} = a \quad y = \theta$$

$$\ddot{\delta} = -B_{22}^{-1}[B_{12}a + n_2(\dot{\theta}, \delta) + K\delta + F\dot{\delta}]$$

The input–output relation from the external reference $a$ to the joint angle $\theta$ is now *linear*, as a result of the inversion control law $u^*$ chosen. The behaviour of this input–output double integration path can be suitably shaped by choosing

$$a = \ddot{\theta}_d + k_v(\dot{\theta}_d - \dot{\theta}) + k_p(\theta_d - \theta)$$

with $k_p > 0$ and $k_v > 0$. The closed-loop control results in

$$u_{\mathrm{CL,PD}} = u^*(\ddot{\theta}_d, \dot{\theta}, \delta, \dot{\delta}) + \frac{1}{d_{11}(\delta)}[k_p(\theta_d - \theta) + k_v(\dot{\theta}_d - \dot{\theta})]$$

Once this feedback control has been applied, an unobservable part related to the dynamics of the elastic variables $\delta$ arises (see also Fig. 2). The stability of this 'sink' plays a crucial role in the proposed control design. In particular, one is interested in the dynamic behaviour of the elastic variables when the trajectory is completed. This describes the way arm vibrations damp out about the final trajectory point, and thus accounts for the positional accuracy of the arm tip.

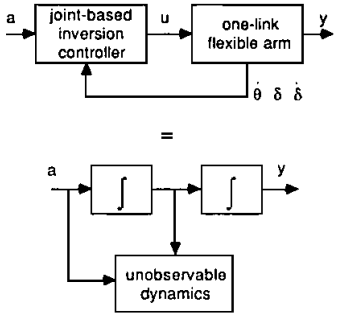


Figure 2. Closed-loop inversion control.

The study of the dynamics of the unobservable part in these conditions is closely related to the so-called 'zero-dynamics' of the given non-linear system (Isidori and Moog 1987). Setting $y(t) \equiv 0$ for all times implies $\dot{y} = \dot{\theta} = 0$ and $\ddot{y} = a = 0$. Replacing these values into the closed-loop dynamics of $\delta$ gives

$$\ddot{\delta} = -B_{22}^{-1}[n_2(0, \delta) + K\delta + F\dot{\delta}] = -B_{22}^{-1}[K\delta + F\dot{\delta}]$$

using the fact that $n_2$ is quadratic in the joint velocity. Note that the internal arm dynamics associated with a constant zero value of the joint output becomes *linear* too. When $F = 0$, since $K$ and $B_{22}$ are positive-definite matrices, the $2m$ eigenvalues are all complex pairs located on the imaginary axis and the system is critically stable. As soon as some passive damping is present, i.e. $F > 0$, these closed-loop roots move to the open left half-plane and asymptotic internal stability is obtained.

The above analysis holds only at the terminal point of the trajectory. Indeed, the elastic deflections must also be kept limited during point-to-point motion in order to

avoid too much stressing of the beam. Note that the deflected configuration of the arm at the end of the trajectory provides the initial conditions for the above linear differential equations governing the residual oscillatory behaviour.

In general, it is quite difficult to extract accurate information about structural damping. Thus, it is reasonable to drop the term $F\dot{\delta}$ from the control law $u^*$. The resulting closed-loop system will be described by

$$\ddot{\theta} = a - D_{12}^{\mathrm{T}}(\delta)F\dot{\delta}$$

$$\ddot{\delta} = -B_{22}^{-1}[B_{12}^{\mathrm{T}}a + n_2(\dot{\theta}, \delta) + K\delta] - D_{22}(\delta)F\dot{\delta}$$

It follows that exact tracking of joint trajectories is no longer guaranteed. The actual trajectory will typically lag behind the desired one by a small amount depending on the modal damping coefficients in $F$. However, the stability properties are preserved.

## 4. Inversion control for a point along the arm

Necessitated by moving towards end-point trajectory tracking, inversion control is investigated next for stiffening the motion of a suitable point along the arm. In fact, there may exist a continuous range of points along the structure, other than just the joint location, for which a smooth trajectory can be exactly reproduced in a stable way (De Luca *et al.* 1988).

The angle $\alpha$ formed by a generic point along the arm with the reference frame can be expressed in parametric form with respect to $\eta$ as (Fig. 1)

$$\alpha(\eta) = \theta + \operatorname{arctg}\left(\frac{w(\eta)}{\eta}\right)$$

For small deflections, the output can be defined as the linearized version of $\alpha$, i.e.

$$y(\eta) = \theta + \frac{w(\eta)}{\eta} = \theta + \frac{\Phi^{\mathrm{T}}(\eta/L)\delta}{\eta}$$

It is worth noting that this parametrization is a convenient one, since for $\eta = 0$ the joint-based strategy of the previous section is recovered, owing to the clamped boundary conditions

$$\lim_{\eta \to 0} \frac{w(\eta)}{\eta} = 0$$

Conversely, for $\eta = L$, a true end-point strategy is obtained.

Applying the inversion algorithm with this output and following the same steps as in the previous case gives

$$\ddot{y} = \left[d_{11}(\delta) + \frac{\Phi^{\mathrm{T}}(\eta/L)}{\eta} D_{12}(\delta)\right][u - n_1(\dot{\theta}, \delta, \dot{\delta})]$$

$$-\left[D_{12}^{\mathrm{T}}(\delta) + \frac{\Phi^{\mathrm{T}}(\eta/L)}{\eta} D_{22}(\delta)\right][n_2(\dot{\theta}, \delta) + K\delta + F\dot{\delta}]$$

The input–output linearizing control is computed as

$$u = n_1(\dot{\theta}, \delta, \dot{\delta}) + \frac{1}{d_{11}(\delta) + \dfrac{\Phi^{\mathrm{T}}(\eta/L)}{\eta} D_{12}(\delta)}$$

$$\times \left[ a + \left( D_{12}^{\mathrm{T}}(\delta) + \frac{\Phi^{\mathrm{T}}(\eta/L)}{\eta} D_{22}(\delta) \right) (n_2(\dot{\theta}, \delta) + K\delta + F\dot{\delta}) \right]$$

$$= u_\eta^*(a, \dot{\theta}, \delta, \dot{\delta})$$

where $a$ is the new control variable. As before, $u_\eta^*$ can be implemented either in an open- or in a closed-loop fashion, with the possible addition of a PD action to increase robustness. Under the above control law, the system equations in the new coordinates $(y, \delta)$ become

$$\ddot{y} = a$$

$$\ddot{\delta} = -\frac{B_{22}^{-1}}{\Gamma(\eta)} [B_{12} a + n_2(\dot{y}, \delta, \dot{\delta}) + K\delta + F\dot{\delta}]$$

with

$$\Gamma(\eta) = 1 - \frac{\Phi^{\mathrm{T}}(\eta/L)}{\eta} B_{22}^{-1} B_{12}$$

which can be obtained after some handy algebraic manipulations.

The stability of the sink, i.e. of the flexible equations, has to be investigated with respect to the parameter $\eta \in [0, L]$. This eventually determines the range of points along the link whose dynamic behaviour can be stiffened. Restricting the study to a local analysis around a given arm configuration, the zero-dynamics is described by

$$\ddot{\delta} = -\frac{B_{22}^{-1}}{\Gamma(\eta)} [K\delta + F\dot{\delta}]$$

The sign of the scalar function $\Gamma(\eta)$ plays a crucial role in the evaluation of the stability properties. Note that $\Gamma(0) = 1$, from which the stability of the joint-based design is again implied. This suggests seeking that value $\eta^*$ at which $\Gamma$ vanishes for the first time. Then, choosing as output a point on the arm at a location $\eta$ in the range $[0, \eta^*)$ guarantees a stable tracking design.

It can be argued that beyond this critical point, application of inversion-based control laws leads to unstable closed-loop behaviour. In the non-linear setting, this is equivalent to the well-known case of non-minimum phase zeros (Chen 1984) that prevent inversion of linear transfer functions. As a consequence, the design of a controller capable of exactly reproducing any smooth trajectory for the arm tip may generally lead to instabilities. This is the case, for instance, in the experimental results reported by Cannon and Schmitz (1986).

## 5. Simulation results

The above inversion control laws have been simulated using a two-mode model of the one-link flexible arm existing in the Flexible Automation Laboratory at the Georgia Institute of Technology. An experimental validation of the model was made by Hastings and Book (1985). In particular, it was found that only two modes are relevant in this case. The arm is 4 ft long and its first two eigenfrequencies are at 2·12 and 14·3 Hz. The equivalent spring coefficients associated with the two assumed modes are $k_1 = 5{\cdot}54$ and $k_2 = 198{\cdot}56$ lbf ft$^{-1}$.

The desired output trajectory specifies an angular motion from $y(0) = 0$ to $y(T) = 90$ deg, with a velocity profile $\dot{y}_d(t) = (90/T)[1 - \cos(360t/T)]$ deg s$^{-1}$, where

$T = 2$ s. The simulations run for four seconds, with a sampling time of one millisecond. This sampling time is estimated to be long enough to perform in real-time the computations required by the most complex of the above controllers. A PD output feedback action is introduced in all simulations with gains chosen as $k_p = 2500$, $k_v = 100$, corresponding to a critical response with a double pole at $-50$.

The conventional PD co-located joint controller was tested first and its tracking performance is shown in Figs 3 and 4. A feedforward acceleration term was then added, which resulted in an order-of-magnitude improvement in the joint tracking (Fig. 5). No significant differences occurred for the end-point tracking, however.

The non-linear inversion-based controllers were applied next. Figures 6 and 7 illustrate the results with the closed-loop control $u_{CL,PD}$ in the case of no passive damping ($F = 0$). The desired joint trajectory is accurately reproduced (0·006 deg as maximum error) with a remarkable improvement in the steady state. The arm tip still oscillates around the final point by less than 0·01 ft; its time evolution does not substantially differ from the one in Fig. 4, and is therefore omitted. Note that some control effort is also present after $T = 2$ s (Fig. 7), and is needed for keeping the joint angle at its desired final value.

Figures 8 and 9 relate to a doubling in value of the load parameters $M_L$ and $J_L$. Some ripples are present in the joint-position error, but the achieved result indicates the robustness of the control scheme with respect to these variations.

The open-loop control $u_{OL,PD}$ has been evaluated for the nominal plant. Although, in this case, the joint maximum error is doubled and the joint angle keeps on oscillating even after $T = 2$ s (Fig. 10), the end-point error is practically the same as in the closed-loop scheme. In addition, the required torque input is very similar. Thus, a cheap implementation of the proposed inversion control law, with no use of deflection measures, is a feasible alternative.

Passive damping in the structure is introduced next with $f_i = 0{\cdot}2(k_i)^{1/2}$, $i = 1, 2$, although this is not compensated in the control law. The benefits are apparent from Figs 11 and 12, which refer to closed-loop control with the same doubling of load parameters as above. A small delay in the tracking of the joint trajectory can be recognized. On the other hand, oscillations in the tip position vanish immediately after the completion of the joint trajectory. In the case of open-loop control, passive damping also has positive effects.

In order to implement inversion-based control for a point along the arm, the assumed-mode shapes of the beam have been computed (Fig. 13). These are essential in determining the range of points that lead to a stable design. Figure 14 shows the distribution of angular accelerations experienced by the arm points at time $t = 0$. The first node occurs at 0·934 ft, which is exactly the value of $\eta^*$ zeroing the function $\Gamma(\eta)$. The points from 0·934 to 3·650 ft are clearly in the opposite phase to the commanded input signal. Note that points in the final range again possess positive angular acceleration, displaying a typical whipping effect. Incidentally, it can be shown that attempting to apply inversion control to such points produces closed-loop instabilities.

On the basis of the previous analysis, the output has been chosen at $\eta = 0{\cdot}9$ ft. The results of Figs 15 and 16 demonstrate the effectiveness of the closed-loop inversion control strategy; angular tracking is satisfactory while the maximum end-point tracking error is halved with respect to the joint-based strategy. The input torque in Fig. 17 is evidence of the control effort after $T = 2$ s necessary to maintain the output at the final target.

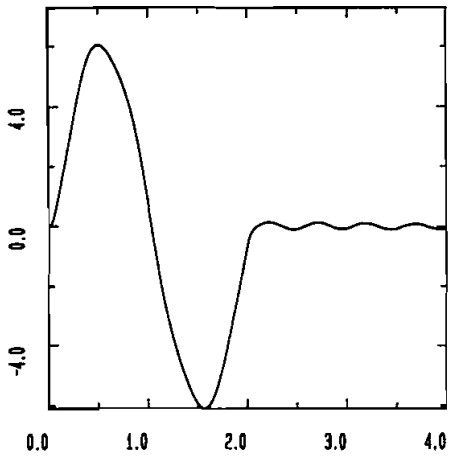


Figure 3. PD control (joint error $\times 10^{-2}$ deg).

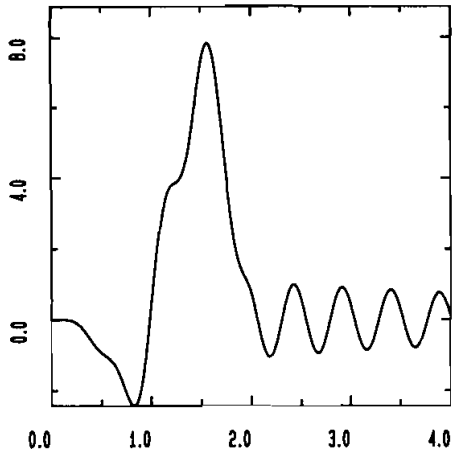


Figure 4. PD control ($x$-component of end-point error $\times 10^{-2}$ ft).

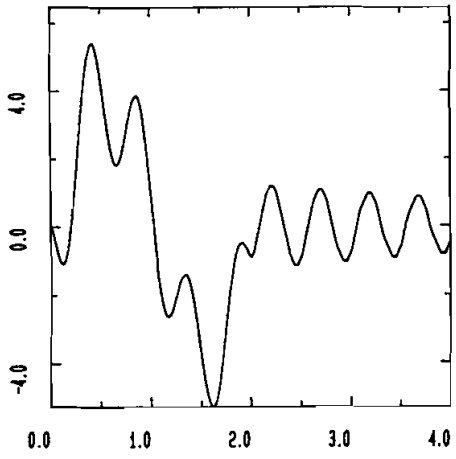


Figure 5. PD control with acceleration feedforward (joint error $\times 10^{-3}$ deg).

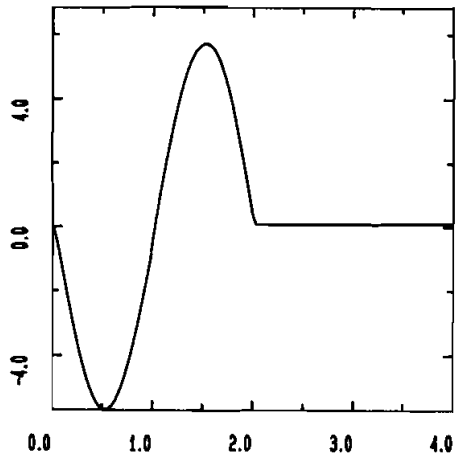


Figure 6. Closed-loop inversion control (joint error $\times 10^{-3}$ deg).

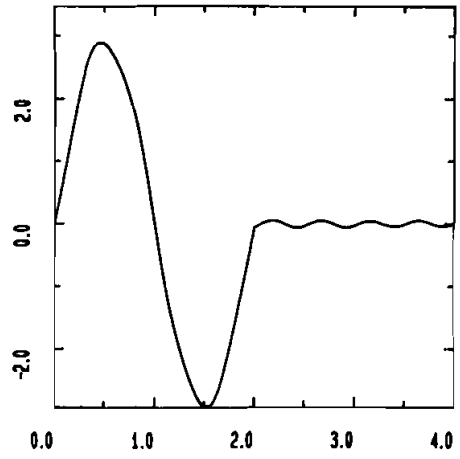


Figure 7. Closed-loop inversion control (input torque: ft lb).

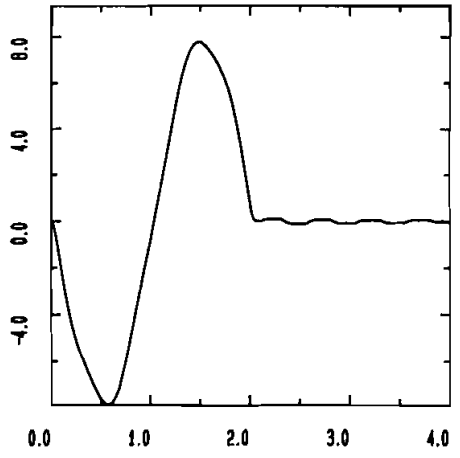


Figure 8. Closed-loop inversion control with double load (joint error $\times 10^{-3}$ deg).

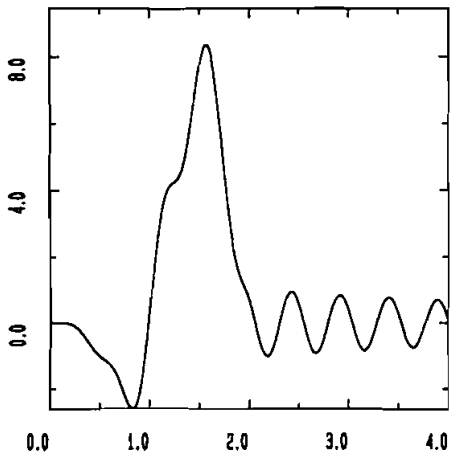


Figure 9. Closed-loop inversion control, double load ($x$-component of end-point error $\times 10^{-2}$ ft).

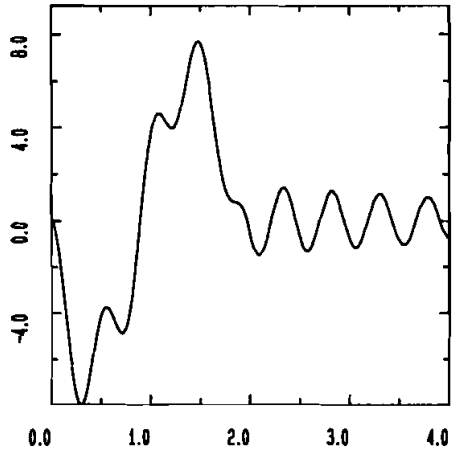


Figure 10. Open-loop inversion control (joint error $\times 10^{-3}$ deg).

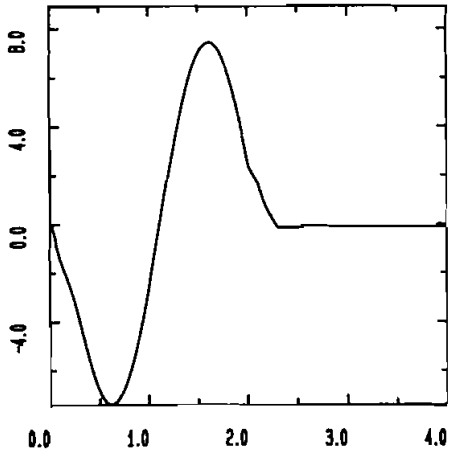


Figure 11. Closed-loop inversion control with double load and $F > 0$ (joint error $\times 10^{-3}$ deg).

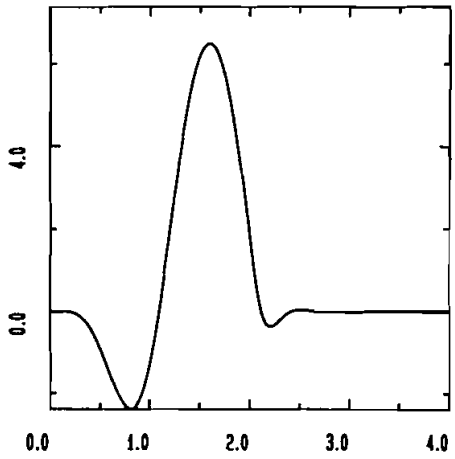


Figure 12. Closed-loop inversion control with double load and $F > 0$ ($x$-component of end-point error $\times 10^{-2}$ ft).

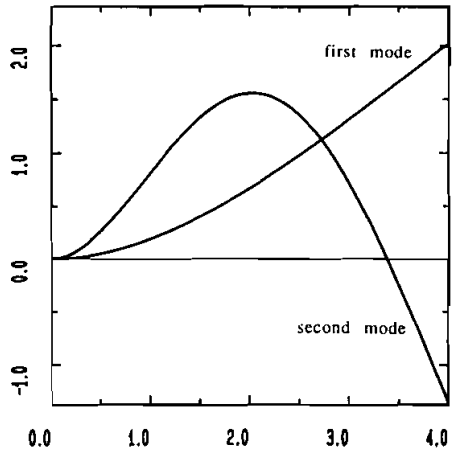


Figure 13. First and second assumed modes shape profiles ($x$-axis: ft).

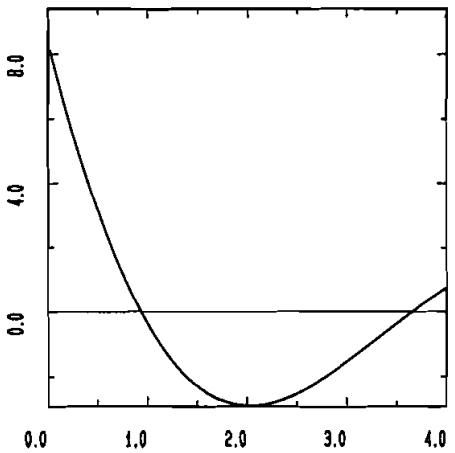


Figure 14. Angular acceleration of the points along the arm at time $t = 0$ ($x$-axis: ft).

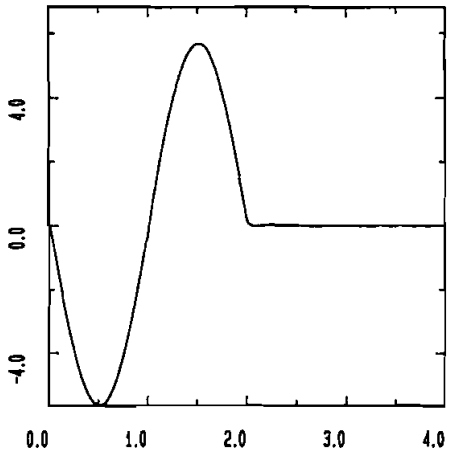


Figure 15. Closed-loop inversion control for a point along the arm with $\eta = 0{\cdot}9$ ft (angular-output error $\times 10^{-3}$ deg).

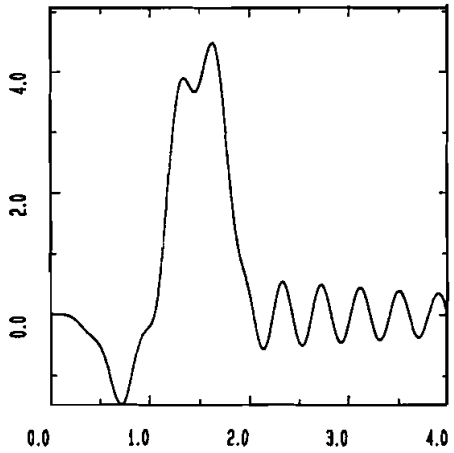


Figure 16. Closed-loop inversion control for a point along the arm with $\eta = 0{\cdot}9$ ft ($x$-component of end-point error $\times 10^{-2}$ ft).

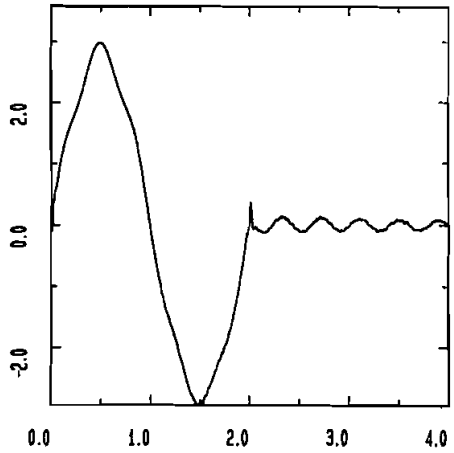


Figure 17. Closed-loop inversion control for a point along the arm with $\eta = 0{\cdot}9$ ft (input torque: ft lb).

Finally, it is interesting to examine the behaviour of the system under closed-loop inversion control for an output chosen in the range of out-of-phase points. For $\eta = 2$ ft, it can be seen from Fig. 18 that the angular error diverges within 5 per cent of the total trajectory time, and so does the input torque in Fig. 19. This can be adduced to the internal instability of the system.

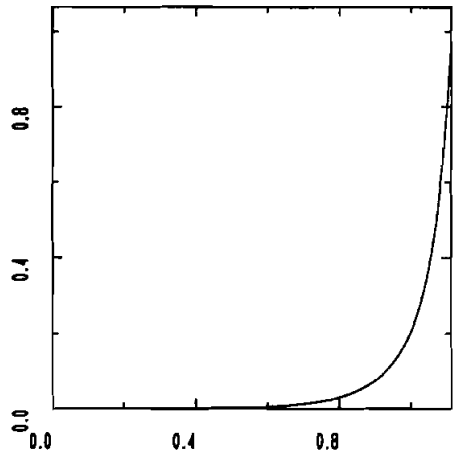


Figure 18. Instability of the closed-loop inversion control for a point along the arm with $\eta = 2{\cdot}0$ ft (angular-output error during the first 0·1 s).

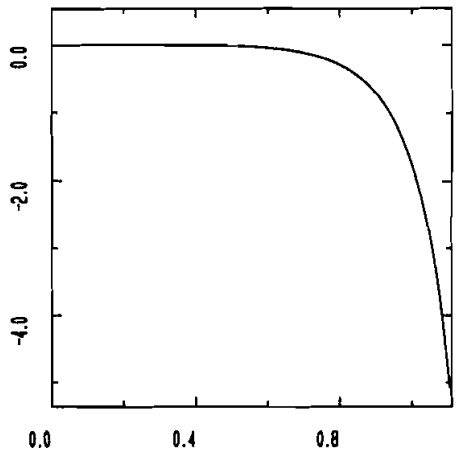


Figure 19. Instability of the closed-loop inversion control for a point along the arm with $\eta = 2{\cdot}0$ ft (input torque during the first 0·1 s).

## 6. Conclusions

Inversion-based controllers have been designed for tracking output trajectories of a one-link flexible arm. It has been shown that any assigned smooth joint trajectory can be exactly reproduced for matched initial conditions. Closed-loop and open-loop schemes have been proposed. If an accurate dynamic model is available, open-loop computation of joint torque plus a linear PD joint-trajectory controller yields satisfactory results. The presence of passive damping considerably improves the

steady-state performance of the above controllers. Although the development has been carried out for a single flexible link, it is possible to extend the joint-based approach to the multi-link case (De Luca and Siciliano 1989).

An alternative strategy has been investigated that allows for the trajectory control of a range of angular outputs defined along the link. Using inversion techniques, it has been shown that the motion of suitable link points can be stiffened; a reduction of end-point deflections has been observed. A proper parametrization of the system output is crucial in discriminating between points leading to stable or to unstable design. As a result, limited confidence should be given to the exact reproduction of end-point trajectories using only inversion techniques. It is believed, however, that the method could serve as a powerful design tool for flexible arms.

## References


BAYO, E., 1987, A finite-element approach to control the end-point motion of a single-link flexible robot. *Journal of Robotic Systems*, **4**, 63–75.

BEJCZY, A. K., 1974, Robot arm dynamics and control. TM 33-669. Jet Propulsion Laboratory, California Institute of Technology, Pasadena, California.

BOOK, W. J., 1984, New concepts in lightweight arms. *Proceedings of the 2nd International Symposium on Robotics Research*, Kyoto, Japan, pp. 203–205.

BOOK, W. J., DICKERSON, S. L., HASTINGS, G., CETIKUNT, S., and ALBERTS, T., 1985, Combined approaches to lightweight arm utilization. *Proceedings of the A.S.M.E. Winter Annual Meeting*, Miami, Florida, pp. 97–107.

CANNON, R. H., JR, and SCHMITZ, E., 1986, Initial experiments on the end-point control of flexible one-link robot. *International Journal of Robotics Research*, **3** (3), 62–75.

CHEN, C. T., 1984, *Linear Systems Theory and Design* (New York: Holt, Rinehart, and Winston).

CRAIG, J. J., 1986, *Introduction to Robotics: Mechanics and Control* (Reading, Mass: Addison-Wesley).

DE LUCA, A., 1988, Dynamic control of robots with joint elasticity. *Proceedings of the I.E.E.E. International Conference on Robotics and Automation*, Philadelphia, Pennsylvania, pp. 152–158.

DE LUCA, A., LUCIBELLO, P., and ULIVI, G., 1988, Inversion techniques for open- and closed-loop control of flexible robot arms. *Proceedings of the 2nd International Symposium on Robotics and Manufacturing Research*, Albuquerque, New Mexico, pp. 529–538.

DE LUCA, A., and SICILIANO, B., 1988, Joint-based control of a nonlinear model of a flexible arm. *Proceedings of the American Control Conference*, Atlanta, Georgia, pp. 935–940; 1989, Inversion-based nonlinear control of robot arms with flexible links. *A.I.A.A. Journal of Guidance and Control*, submitted for publication.

ENGELBERGER, J. F., 1980, *Robotics in Practice* (London: Kogan Page).

HASTINGS, G. G., and BOOK, W. J., 1985, Experiments in optimal control of a flexible arm. *Proceedings of the American Control Conference*, Boston, Massachusetts, pp. 728–729.

HIRSCHORN, R. M., 1979, Invertibility of multivariable nonlinear control systems. *I.E.E.E. Transactions on Automatic Control*, **24**, 855–865.

ISIDORI, A., and MOOG, C. H., 1987, On the nonlinear equivalent of the notion of transmission zeros. *Modeling and Adaptive Control*, edited by C. I. Byrnes and K. H. Kurszanski (Berlin: Springer-Verlag).

MEIROVITCH, L., 1967, *Analytical Methods in Vibrations* (New York: Macmillan).

NICOSIA, S., TOMEI, P., and TORNAMBÈ, A., 1989, Nonlinear control and observation algorithms for a single-link flexible robot arm. *International Journal of Control*, **49**, 827–840.

SICILIANO, B., and BOOK, W. J., 1988, A singular perturbation approach to control of lightweight flexible manipulators. *International Journal of Robotics Research*, **7** (4), 79–90.

SICILIANO, B., YUAN, B. S., and BOOK, W. J., 1986, Model reference adaptive control of a one link flexible arm. *Proceedings of the 25th I.E.E.E. Conference on Decision and Control*, Athens, Greece, pp. 91–95.

SINGH, S. N., and SCHY, A. A., 1984, Robust torque control of an elastic robotic arm based on invertibility and feedback stabilization. *Proceedings of the 24th I.E.E.E. Conference on Decision and Control*, Las Vegas, Nevada, pp. 1317–1322.